Measurements of Inelastic Scattering of 661.7 KeV Photons by Electrons

Yongao Hu*
MIT Department of Physics

(Dated: April 7, 2025)

This report presents the results of the Compton scattering experiment conducted in MIT Junior Lab during Spring 2025. The experiment was successful in demonstrating the angular dependence of energy of the scattered photons and recoiled electrons, as well as the angular dependence of scattering rate. The experiment also measured the total cross section of the Compton scattering process. The results of the experiment are consistent with the theoretical predictions treating photons as particles.

I. INTRODUCTION

Compton scattering, discovered by Arthur Compton in 1923, is the inelastic scattering of a photon by a charged particle, usually an electron [1]. If we treat light as waves, the wavelength of the light should not change when it scatters off an electron. However, if we treat light as particles, we expect energy shift of the scattered photons compared to incident photons.

In this experiment, we will measure three variables to verify the particle nature of light: the energy of the scattered photons as a function of the scattering angle, the scattering rate of scattered photons at each angle, as well as total cross section [4].

II. THEORY: RELATIVISTIC SCATTERING OF PHOTONS

II.1. Relativistic Kinematics of Scattering

In classical wave theory, there is no mechanism to change the wavelength of light when it scatters off an electron [3]. However, if we treat the photon as a particle with energy $E = hf$ and momentum $p = hf/c$, we can use the conservation of energy and momentum to calculate the shift in energy of the photon when it scatters off an electron [5]. We can calculate the energy of the scattered photon [5]:

$$E_f = \frac{E_i}{1 + \frac{E_i}{m_e c^2}(1 - \cos\theta)} \tag{1}$$

where E_i is the energy of the incident photon, E_f is the energy of the scattered photon, and θ is the scattering angle.

II.2. Scattering Rate

We can calculate the angular dependence of the scattering rate by measuring the differential cross section. The differential cross section $\frac{d\sigma}{d\Omega}$ is the probability of the scattering process occurring in a solid angle $d\Omega$. Classically, the differential cross section of the Compton scattering process is given by the *Thomson scattering* formula which describe the elastic scattering of electromagnetic radiation by a free charged particle (in this case, an electron) [3]:

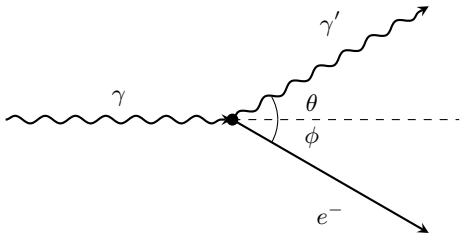

FIG. 1. Compton scattering diagram showing the incident photon (γ), the scattered photon (γ') deflected by an angle θ, and the recoil electron (e^-) at an angle ϕ.

$$\frac{d\sigma}{d\Omega} = r_0^2 \left(\frac{1 + \cos^2\theta}{2}\right) \tag{2}$$

where $r_0 = \frac{e^2}{4\pi\epsilon_0 m_e c^2}$ is the classical electron radius [7]. However, we need to include the relativistic effects when the energy of the photon is comparable to the rest mass of the electron. If we include the relativistic effects, the differential cross section of the Compton scattering process is given by the *Klein-Nishina formula* [6]:

$$\frac{d\sigma}{d\Omega} = \frac{r_0^2}{2}\left(\frac{E_f}{E_i}\right)^2 \left(\frac{E_f}{E_i} + \frac{E_i}{E_f} - \sin^2\theta\right) \tag{3}$$

II.3. Total Cross Section

We also measure the total cross section of the scattering. We measure the attenuation of the photon beam as a function of the thickness of the absorber. We can then fit a decaying exponential function to the data to calculate the total cross section [4].

$$A = A_0 e^{-\mu l} = A_0 e^{-\sigma N \rho l} \tag{4}$$

* yongao@mit.edu

where μ is the attenuation coefficient of the absorber and l is the thickness of the absorber. ρ is the density of the attenuator, N is the number of electrons per unit mass.

We can compare the measured total cross section with the theoretical prediction. According to Thomson scattering, the total cross section of the Compton scattering process is given by [3, 6]:

$$\sigma = \frac{8\pi}{3} r_0^2 \approx 66.5 \text{ fm}^2 \tag{5}$$

And according to the Klein-Nishina formula, the total cross section of the Compton scattering process is given by [6] as a function of the energy of the incident photon:

$$\sigma = 2\pi r_e^2 \left[\frac{1+x}{x^3} \left(\frac{2x(1+x)}{1+2x} - \ln(1+2x) \right) + \frac{\ln(1+2x)}{2x} - \frac{1+3x}{(1+2x)^2} \right] \tag{6}$$

where $x = \frac{E_i}{m_e c^2}$.

III. EXPERIMENTAL DESIGN AND DATA ANALYSIS

III.1. Apparatus

The source of the photons is a ^{137}Cs radioactive source. The source emits photons with energy $E_i = 661.6$ keV [4] to scatter off electrons in NaI scintillator. The electrons can be approximated as free electrons due to the high energy of the incident photons. The experiment uses two scintillation detectors. One scintillator, the "recoil detector", is used as the target to scatter photons and measure the energy of the recoiled electrons, while the other scintillator, the "scatter detector", is used to detect and measure the energy of the scattered photons. The scatter detector is placed at an angle θ with respect to the incident photon beam.

To make sure that we are not measuring the energy of the photons from the source, we will use a coincidence circuit to amplify and measure the energy of the scattered photons and recoiled electrons [4]. The circuit diagram is shown in Fig. 2. The coincidence circuit will only output a signal when both detectors detect a photon within a short time window. We feed the output from the scintillators into pre-amplifiers and amplifiers. The outputs of the amplifiers are connected to multichannel analyzers (MCA), with 2048 equally spaced energy channels, to measure the energy of the scattered photons and recoiled electrons. The outputs of the amplifiers are also fed into a coincidence circuit: we first use inverters and discriminators to covert the pulses above a certain threshold from the amplifiers into square waves to reduce noise. The discriminated square waves are then fed into a coincidence circuit. The output of the coincidence circuit is connected to a delay generator to ensure that MCA has enough time to record the energy of the scattered photons and recoiled electrons. The output of the delay generator is connected to the gates of MCA to ensure that we are only measuring the energy from Compton scattering events and not from the source or stray radiation [4].

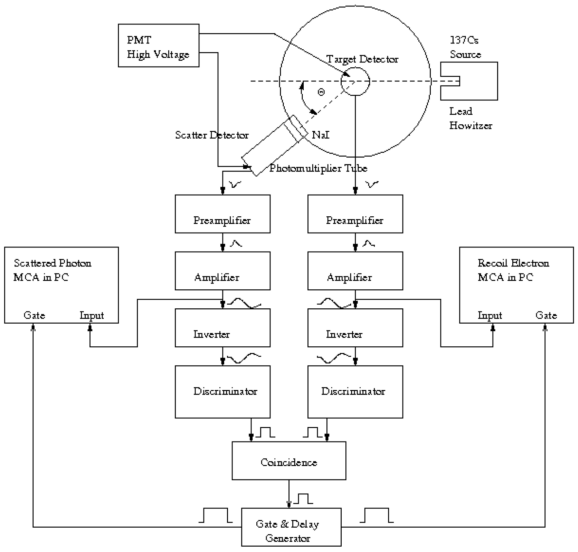

FIG. 2. Circuit diagram of the Compton scattering experiment. The circuit uses a coincidence circuit to measure the energy of the scattered photons and recoiled electrons.

III.2. Peak Fitting

In order to find the peak of energy of the detected particles, we first use a Kernel Density Estimator (KDE) to smooth the data: we use a Gaussian kernel with a bandwidth of 10 keV. KDE fits a Gaussian function to each data point and then sums up the Gaussian functions to create a smooth curve. We use KDE to preliminarily find the peak of the energy of the detected particles.

We then use a peak-finding algorithm to find the peak and valley of the energy of the detected particles. Afterwards, we fit a Gaussian function to the original data between the two adjacent valleys to find the peak. The uncertainty of the peak is the width of the Gaussian function.

The area under the Gaussian function is proportional to the number of detected particles that we considered as "detected" by the detector. Here, we use the area between half of the peak and the peak as the area of the Gaussian function (Full Width at Half Maximum, FWHM). In order to find the uncertainty of FWHM, we first use KDE smoothed data to find the bin of KDE where half of the peak is located. We then use a Monte Carlo method to find the uncertainty of the FWHM: we use the original data within the bin of KDE where half of the peak is located to find the number of count and the standard deviation of the number of count at half

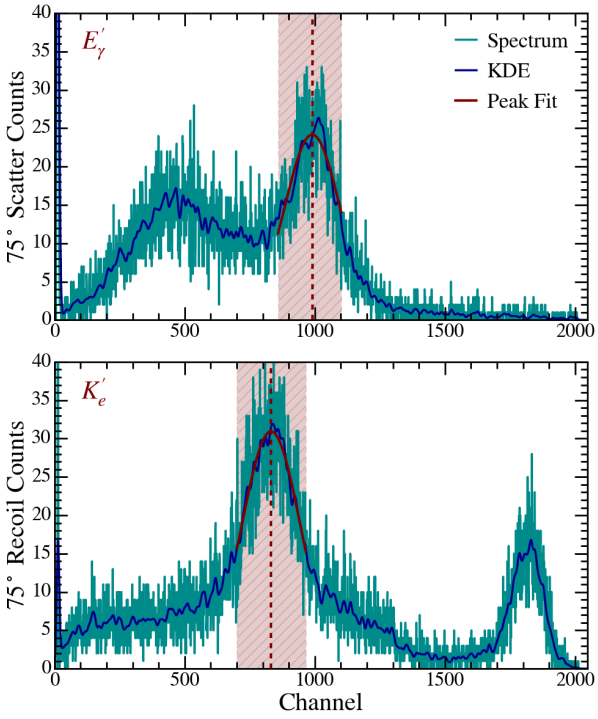

FIG. 3. Peak-fitting algorithm to find the peak of the energy of the detected particles. The green curve is the original data and the blue curve is the KDE smoothed data. The vertical red dotted lines are the peaks of the KDE smoothed data. The red curve is the Gaussian function fitted to the peaks of the data. The shaded area is the FWHM of the gaussian fits. Here we present both a scatter spectrum (top) and a recoil spectrum (bottom).

maximum. We then randomly sample using a normal distribution with the mean of the number of count and the standard deviation of the number of count to fit a Gaussian function to the sampled data. We repeat this process to find the standard deviation of the FWHM.

We can see the peak-fitting algorithm in Fig. 3.

III.3. Calibration

As we do not know exactly what each bin of MCA correspond to in terms of energy, we need to calibrate the MCA. We use a ^{22}Na source and a ^{133}Ba source, with known gamma ray peaks, to calibrate the MCA [2]. After identifying the peak of the energy from the calibration sources, we fit a linear function between the channel number of the MCA and the energy of the gamma rays. Note that we calibrate the detectors separately as they have different gains. We also calibrate them at the beginning of different sessions to account for the drift of the gains. The calibration result is shown in Fig. 4.

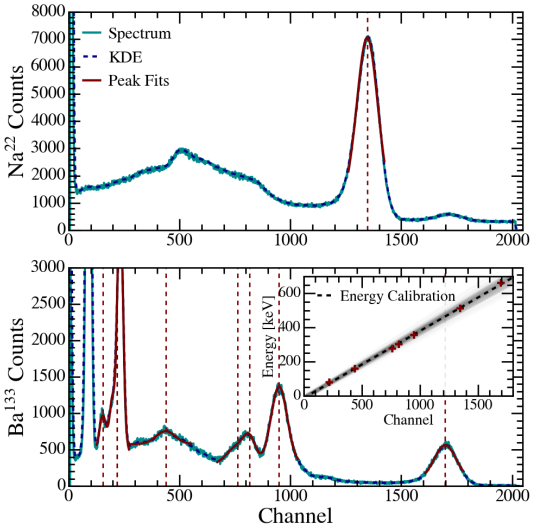

FIG. 4. Calibration of the circuit using ^{22}Na and ^{133}Ba sources. We use the peakfinding algorithm to find peaks of the two sources and fit a linear function between the channel number of the MCA and the energy of the gamma rays. The grey area of the fitting plot is the uncertainty of the fitting.

III.4. Angular Dependence of Scattering

We measure the energy of the scattered photons as a function of the scattering angle θ. We place the scatter detector at different angles with respect to the incident photon beam and measure the energy of the scattered photons. After finding the peak of energy of the scattered photons at different angles, we can overlay them with theoretical predictions to verify the Compton scattering formula.

We also measure the total collection time of the scattered photons and recoiled electron at each angle to calculate the scattering rate at each angle .We can overlay the rate of the recoiled electrons with the Thomson scattering formula and Klein-Nishina formula to verify the angular dependence of cross section of the Compton scattering process.

III.5. Total Cross Section Measurement

We measure the attenuation of the photon beam as a function of the thickness of the absorber. In particular, we are using 4 types of plastic absorbers with roughly 1:1 carbon:hydrogen ratio [4]. We place absorbers of different thicknesses in the path of the photon beam and measure the attenuation of the photon beam using the scatter detector. We fit an exponential decaying function to the data of the attenuation of the photon beam as a function of the thickness of the absorber [4].

IV. RESULTS

IV.1. Angular Dependence of Scattering

At $\theta = 0$, theory predicts that the energy of the scattered photon is the same as the incident photon. However, due to alignment errors, our measurement of the energy of the scattered photon at $\theta = 0$ is not exactly the same as the incident photon. We used the energy of the scattered photon at $\theta = 0$ to fit the offset of the angular measurement, which is determined to be $(2.56 \pm 0.71)^\circ$. The systematical uncertainty of the angle measurement is 0.5° which comes from the resolution of the angle measurement. The result is shown in Fig. 5.

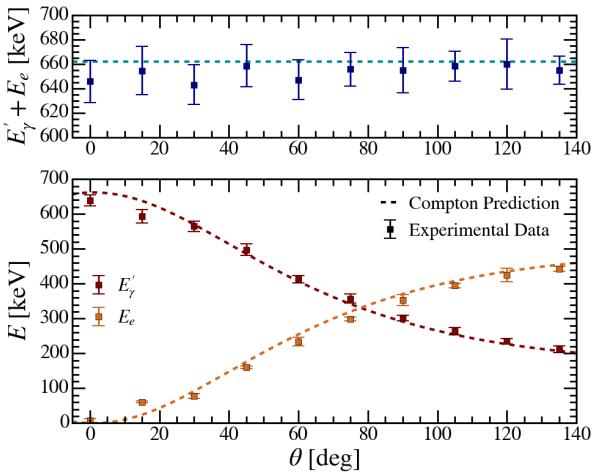

FIG. 5. Angular dependence of the energy of the scattered photons and recoiled electrons. The angular uncertainty is 0.5° which is the resolution of the angle measurement. We can see that the energy of the scattered photons decreases with the scattering angle, while the energy of the recoiled electrons increases with the scattering angle. We can calculate the total energy of the scattered photons and recoiled electrons at each angle to verify that their total energy is the same as the incident photon of 661.6 KeV.

The statistical error of the energy measurement comes from the standard deviation from the peak-fitting algorithm.

We can see that the total energy of the scattered photons and recoiled electrons at each angle is within the error of the incident photon energy, but all slightly lower than the incident photon energy. We can attribute it to be a systematic error due to the attenuation of the photon beam due to the air between the source and the detector.

IV.2. Angular Dependence of Scattering Rate

We can see the angular dependence of the scattering rate in Fig. 6. We can see that the scattering rate decreases with the scattering angle, which is consistent with Klein-Nishina formula.

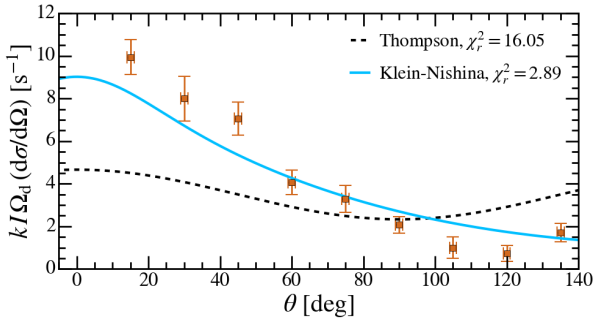

FIG. 6. Angular dependence of the scattering rate of the Compton scattering process. The angular uncertainty is 0.5° which is the resolution of the angle measurement.The scattering rate decreases with the scattering angle, which is consistent with the Klein-Nishina formula and not the Thomson formula.

Note that the statistical error of the data comes from the standard deviation from the peak-fitting algorithm.

Due to the method we chose to measure the scattering rate, we are losing the scattering rate of the photons on the compton continuum [4], where scattered photons have lower energy than the peak energy. However, we can see from Fig. 3 that the recoil spectrum of recoil electron just have one singular peak. This is because the recoil electron has a much larger mass than the photon, so the recoil electron has a much smaller energy spread than the scattered photon. As the number of recoil electrons should be the same as the number of scattered photons because of the coincidence circuit, we use the recoil electron to measure the scattering rate.

Due to the finite size of the detectors and that it covers more than one angle, we have a systematic error in the measurement of the scattering rate. Hence, this graph is more of a qualitative representation of the angular dependence of the scattering rate.

IV.3. Total Cross Section

We can see the attenuation of the photon beam as a function of the thickness of the absorber in Fig. 7. We can fit an exponential decaying function to the data to calculate the total cross section of the Compton scattering process.

The statistical error of the data comes from the standard deviation from the peak-fitting algorithm. The systematic error of the data comes from resolution of dimension measurement as well as mass measurement. We propagate these error to the fitting parameters to find the uncertainty of the total cross section. We can see that the total cross section of the Compton scattering process is consistent with Klein-Nishina formula within 1σ and not the Thomson formula.

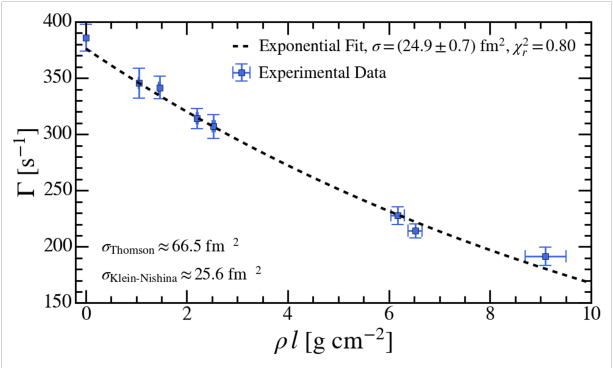

FIG. 7. Attenuation of the photon beam as a function of the mass density times thickness of the absorber. We can fit an exponential decaying function to the data to calculate the total cross section of the Compton scattering process.

V. CONCLUSION

The Compton scattering experiment successfully demonstrated the particle nature of light. The experiment measured the energy of the scattered photons and recoiled electrons as a function of the scattering angle. The experiment also measured the total cross section of the Compton scattering process. The results of the experiment are consistent with the theoretical predictions of Klein-Nishina formula, treating photons as particles.

ACKNOWLEDGMENTS

The author gratefully acknowledges their lab partner V. Tran for their invaluable assistance. The author also thanks the 8.13 teaching team for their guidance in the lab. This work was supported by the MIT Department of Physics.

[1] A. H. Compton. A quantum theory of the scattering of x-rays by light elements. *Physical Review*, 21:483–502, 1923.
[2] R. L. Heath. Scintillation spectrometry. gamma-ray spectrum catalogue. 2nd edition. volume 1 of 2. Technical report, Phillips Petroleum Co. Atomic Energy Div., Idaho Falls, Idaho, 08 1964.
[3] J. D. Jackson. *Classical electrodynamics; 2nd ed.* Wiley, New York, NY, 1975.
[4] MIT Department of Physics. Compton scattering. https://mitx.mit.edu, August 2023. MIT Junior Lab Experiment Documentation.
[5] D. Morin. *Introduction to Classical Mechanics: With Problems and Solutions*. Cambridge University Press, 1st edition, 2008.
[6] S. Weinberg. *The Quantum theory of fields. Vol. 1: Foundations*. Cambridge University Press, 6 2005.
[7] B. Zwiebach. *Mastering Quantum Mechanics: Essentials, Theory, and Applications*. The MIT Press, 2022.